2018 IEEE Intelligent Vehicles Symposium (IV)
Changshu, Suzhou, China, June 26-30, 2018

Coding Pavement Lanes for Accurate Self-localization of Intelligent Vehicles

Qianwen Tao, Zhaozheng Hu*, Hao Cai, Gang Huang and Jie Wu

Abstract— **Self-localization is a key technology for intelligent vehicles. This paper demonstrates a practical and easy solution to vehicle self-localization by simply coding pavement lane lines. Especially, the coding of pavement lane lines makes it possible to distinguish unique pavement marking within certain ranges, which is crucial for vehicle localization. Based on the coded pavement lane lines, we proposed a multi-scale strategy for accurate vehicle localization. The localization method consists of coarse localization with Real-time Locating Systems (RTLS), marking-level localization with marking matching, and metric localization by matching distinctive visual feature points around the marking area. The proposed method has been tested by using the actual data collected in the field, where we encoded the pavement lane lines with two different colors (i.e., white and yellow). The results demonstrate that the proposed method can achieve sub-meter localization accuracy by referring to the coded pavement lane lines. The results also demonstrate that advanced road infrastructure could greatly support intelligent vehicles with low-cost and reliable solutions.**

I. INTRODUCTION

A typical intelligent vehicle usually consists of the modules of perception, decision making, path planning, and control. Vehicle self-localization, which is the process of determining the position and the pose of the vehicle, is crucial for all the above modules.

From the literatures, existing vehicle self-localization methods can be generally classified into three categories. The first category is for the Global Positioning System (GPS) related methods. As raw GPS receivers only provide low positioning accuracy (e.g., as low as 10-meter accuracy or less), it is not feasible for direct intelligent vehicle applications. Usually, GPS is integrated with other sensors (i.e., Inertial Measurement Unit (IMU), Real-time Kinematic (RTK), etc.) for more accurate accuracy. For example, the integration of GPS and IMU can yield less than 10cm positioning errors [1]. The Differential GPS (D-GPS) methods can also reach high position accuracy (i.e., 5cm or less) based on the base stations. And one popular approach is the RTK methods [2]. However, these methods are usually very costly in practice. And they all suffer from the GPS-blind problems, especially in urban environments. Hence, many researchers propose using the Real-time Locating Systems (RTLS) to identify and track the location of vehicles in real time. These methods may utilize WiFi [3], Ultra-Wideband (UWB) [4], Blue Tooth [5], etc., for real-time positioning. The second category is for the vision-based localization methods, which are based on the low-cost cameras [6-10]. One popular method is to use a monocular camera for lane detection, therefore to compute the relative position between the camera and the lanes [6, 7]. However, only traverse position is computed for vehicle self-localization. And some methods try to integrate the pavement marking and High Definition (HD) map for vehicle positioning [8, 9]. However, as natural pavement markings are sparely distributed and high repetitive, these methods are not practical enough in the field. Vision odometry or Simultaneous Localization and Mapping (SLAM) methods are also applied in vehicle self-localization [10]. However, vision odometry has serious drift error problem, which is vital for open road scenarios. And vision SLAM methods suffer from the poor robustness in front-end loop closure detection and the complicated after-end optimization. Recently, some localization methods based on pre-stored visual maps are developed. The last category is for the LiDAR based localization methods. One state-of-the-art method was proposed by Apollo team by using a Velodyne HDL-64E. They used LiDAR data for map generation and localized the vehicle by matching LiDAR data in cell-grid scale with 5-10cm accuracy [11]. However, such method relies on the high-cost laser hardware.

From the literature review, most existing methods solely rely on the sensed data (i.e., GPS, image, LiDAR, etc.) for vehicle localization, which usually leads to high cost, low accuracy, and poor robustness in practice. In this paper, we suggest a novel solution to vehicle self-localization by coding the pavement lanes. We demonstrate that the problem of vehicle localization can be greatly simplified if the pavement lane lines are well encoded in different colors. In addition, a more reliable and accurate method for vehicle localization can be developed based on the coded pavement lanes. Contributions of this paper are twofold. First, we proposed using pavement lane coding in support of intelligent vehicle localization. We can thus distinguish unique pavement marking within certain ranges by coding pavement lane lines in different colors for accurate localization. Second, based on the coded pavement lanes, we proposed a multi-scale strategy for accurate vehicle localization, which consisted of RTLS-based coarse localization, marking-level localization, and finally metric localization by matching visual points around the marking areas.

II. THE PROPOSED METHOD

The proposed vehicle localization method is illustrated in Fig. 1. Based on a database of WiFi fingerprints, images and ground truths of all roads collected by visual map created vehicle, the method consists of three steps. First, a certain range area is derived from coarse localization, which can determine the unique pavement marking. Second, after the

The authors are with Intelligent Transportation Systems (ITS) Research Center, Wuhan University of Technology, Wuhan 430063, China. Correspondence author email: zzhu@ whut.edu.cn.

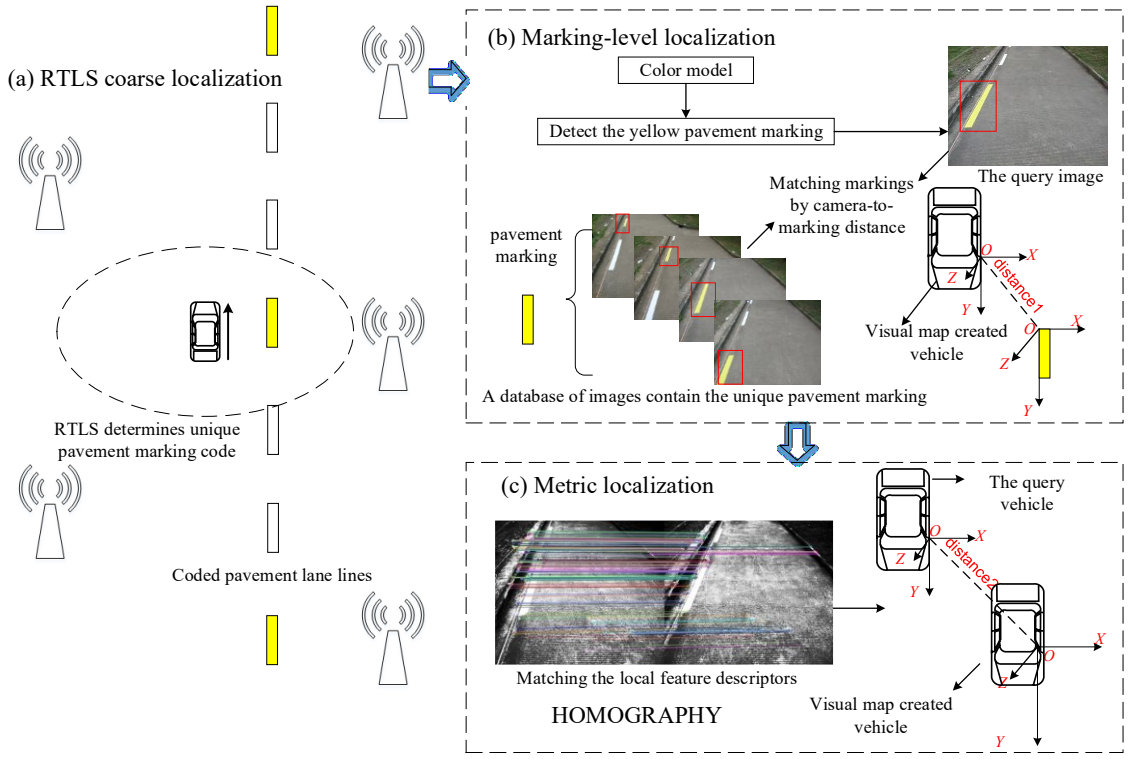

Figure 1. Vehicle localization by referring to the coded pavement lane lines: (a) coarse localization with RTLS; (b) marking-level localization by matching marking; (c) metric localization by matching distinctive visual feature points around the marking area.

yellow pavement marking in the query image is detected by a color model, the nearest map image can be chosen from map images which contain the unique pavement marking by marking-level localization. Third, local feature descriptors of the nearest map image and the query image are extracted to match for further refining localization result by metric localization.

A. Pavement Lane Coding for Localization

Coding pavement lanes is for the purpose of vehicle localization. As shown in Fig. 2(a), a typical dash lane consists of a sequence of squares in white color. As these squares have identical shapes and colors, it is impossible to distinguish them for localization purpose. However, if we code part of the squares in a different color (i.e., yellow), as shown in Fig. 2(b), it may be possible to derive a unique marking, e.g., a coded yellow square, within a range distance (also see in Fig. 1).

In practice, we can take different coding strategies, such as color coding, texture coding, size coding, etc. (see Fig. 2(b)). In this paper, we code lanes in two different colors of white and yellow such that these two different colors appear in sequence. In this paper, we try to code one square in yellow from a number of E squares. Based on the standards, the geometric parameters for a typical highway road are demonstrated in Fig. 4 (a).

Let r denote the uncertainty from the coarse localization. We can hence compute the number E with the following equation

$$E = CEIL\left(\frac{2r}{d_L + d_a}\right), \tag{1}$$

where $CEIL(.)$ is the ceiling function, and d_L and d_a are the lane line distance and the separation distance between two lane lines, respectively. Such color coding allows us to distinguish a unique yellow square from the coarse localization, therefore for vehicle localization. It is obvious that an appropriate r can solve the ambiguity of matching the query image with the image database.

B. Coarse Localization with RTLS

As there were many GPS blind areas in urban cities, we proposed using a WiFi fingerprint strategy for vehicle coarse localization. The WiFi access points (AP) can be evenly

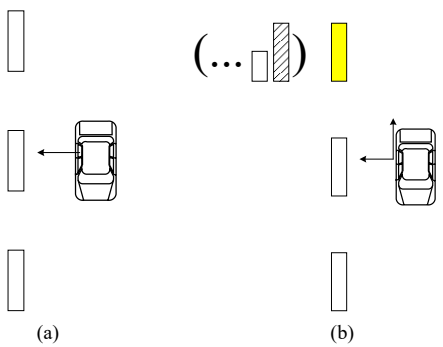

Figure 2. Pavement lane coding in two colors for vehicle localization: (a) conventional lanes; (b) coded lanes in colors.

distributed along the roadside. Before localization, a WiFi fingerprint map should be established. The map is a lookup table, which describes the positions and the corresponding WiFi fingerprint. A WiFi fingerprint consists of the MAC addresses of all the accessible APs, and the corresponding RSSI values as follows

$$W_i = \left\{ \left(M_1, R_1\right), \left(M_2, R_2\right), \ldots\ldots, \left(M_{m_i}, R_{m_i}\right) \right\}, \quad (2)$$

where M represents the AP MAC address, R for RSSI, and m_i for the number of WiFi collected from the i^{th} site. In the step of localization, the collected WiFi fingerprint at each step is matched with those in the map to retrieve the vehicle position. In this paper, we proposed a novel matching, which takes the MAC address matching and RSSI matching into accounts as follows

$$L\left(x, y\right) = N \ln\left(1+\lambda\right) - \sum_{i=1}^{N} \left(\frac{x_i - y_i}{x_i} \right)^2, \quad (3)$$

where N is the number of MAC addresses, x_i and y_i are for the RSSI of the current WiFi and the RSSI of WiFi in the map which are corresponding to the i^{th} MAC address matched, and $\lambda \geq 0$ is an empirical value. With (3), we can find a number of fingerprints with the least $L(x, y)$ in the map such that coarse localization is derived afterwards.

C. Marking-Level Localization by Marking Matching

From the coarse localization result, we can derive a certain range area, within where all the images in the map are chosen as candidates. The marking-level localization step tries to retrieve one map image from the candidates that is nearest to the query image. To serve this purpose, we need to realize two steps: a) develop a statistical color model (SCM) to extract and detect yellow pavement markings, a step called pavement marking detection; b) match the coded yellow square from the query image with those from the candidates, a step called pavement marking matching in this paper.

a) Pavement Marking Detection

We proposed using a SCM to extract and detect yellow pavement markings from images. As yellow markings have different color values due to different lighting conditions and road environments, we need to model such color distributions for color analysis.

We try to train a Gaussian SCM (G-SCM) for color analysis by using a large number of pixel colors that are extracted from the actual video log images. To achieve more reliable representation, we first transform the color space of Red-Greed-Blue (RGB) to Hue-Saturation-Value (HSV). The proposed G-SCM consists of a 3×1 vector to represent the mean value and a 3×3 matrix for the covariance of the color samples. The 3×1 mean value vector is computed as follows

$$\mu = \left[E\left(H\right) \quad E\left(S\right) \quad E\left(V\right) \right]^T, \quad (4)$$

where H, S, V are hue, saturation, and value components of all the training color samples, and $E(H)$, $E(S)$ and $E(V)$ are the means of them, respectively. The 3×3 covariance matrix C is also computed as follows

$$C = \begin{bmatrix} v\left(H,H\right) & v\left(H,S\right) & v\left(H,V\right) \\ v\left(S,H\right) & v\left(S,S\right) & v\left(S,V\right) \\ v\left(V,H\right) & v\left(V,S\right) & v\left(V,V\right) \end{bmatrix}, \quad (5)$$

where the function $v(X,Y)$ takes the forms as

$$v\left(X,Y\right) = E\left[\left(X - E\left(X\right)\right)\left(Y - E\left(Y\right)\right) \right]. \quad (6)$$

From the G-SCM, we can compute the probability or the likelihood that an input color is yellow as follows

$$G\left(I\right) = \frac{1}{\left(2\pi\right)^{3/2} \left|C\right|^{1/2}} \exp\left(-\frac{\left(I-\mu\right)^T C^{-1} \left(I-\mu\right)}{2} \right), \quad (7)$$

where I is pixel value of each point in the image, a 3×1 matrix.

In practice, we can modify the above equation for easy computation as follows

$$G\left(I\right) \propto \left(I-\mu\right)^T C^{-1} \left(I-\mu\right). \quad (8)$$

With the proposed G-SCM model, we can segment and highlight all the yellow colors in the images. As a result, the color segmentation results can be integrated with the conventional line extraction and tracking methods for yellow pavement marking detection.

b) Marking Matching

The detection of yellow pavement makings thus allows us to narrow down the candidates such that only those candidates with yellow markings are selected. Also, from the detected lane lines and vertices, we can compute the distance between the camera and the pavement marking by using some conventional methods [12, 13]. The computed camera-to-marking distance can be used as clue to refine marking matching. From the map, we can compute the camera-to-marking distances from all the candidate images derived from the detection step. As a result, we can derive a unique map image, which has the least distance difference between the distance computed from the query image and those from the candidate images from the maps.

D. Metric Localization

As we use marking-level localization to derive a unique map image by marking matching, metric localization is finally applied to further refine the localization result by matching the distinctive visual feature points around the marking area. Due to the real-time positioning requirement, we proposed a fast method to match the query image and the unique map image by using the well-known local feature descriptors of ORB (Oriented FAST Rotated BRIEF) [14]. First, a sufficient number of ORB feature points are extracted from the query

image. Note that all the feature points are extracted in advance and stored for all the images in the map. Hence, we can directly match the local features between the query and the candidate images. In practice, we also apply the Random Sample Consensus (RANSAC) [15] method to remove outliers to enhance the matching robustness. Finally, if there are sufficient numbers of feature points matched between the two images, it is believed that the pavement marking matching is correct.

From the matched feature points, also called point correspondences, we can relate the two images by a homography as follows [12]

$$\begin{bmatrix} u_q & v_q & 1 \end{bmatrix}^T \cong H_q \begin{bmatrix} u_m & v_m & 1 \end{bmatrix}^T . \quad (9)$$

And from the mapping process, the homography H_m between the physical plane (i.e., pavement plane) and the map image is computed from the calibration step as follows

$$\begin{bmatrix} X & Y & 1 \end{bmatrix}^T \cong H_m \begin{bmatrix} u_m & v_m & 1 \end{bmatrix}^T . \quad (10)$$

By combing (9) and (10), we can derive the homography between the physical plane and the query image as follows

$$\begin{bmatrix} u_q & v_q & 1 \end{bmatrix}^T \cong H_q H_m^{-1} \begin{bmatrix} X & Y & 1 \end{bmatrix}^T \cong H \begin{bmatrix} X & Y & 1 \end{bmatrix}^T . \quad (11)$$

From projective geometry, the homography can be expressed with the camera calibration matrix K, the rotation R, and the translation t, as follows [12]

$$H \cong K \begin{bmatrix} r_1 & r_2 & t \end{bmatrix}^T , \quad (12)$$

where r_i is the i^{th} column vector of R. Therefore, the pose of the vehicle-borne camera with respect to the coded pavement lane is computed as follow [12]

$$R = \left[\frac{K^{-1}h_1}{\left\| K^{-1}h_1 \right\|} \quad \frac{K^{-1}h_2}{\left\| K^{-1}h_2 \right\|} \quad \frac{K^{-1}h_1}{\left\| K^{-1}h_1 \right\|} \otimes \frac{K^{-1}h_2}{\left\| K^{-1}h_2 \right\|} \right], \quad (13)$$

$$t = \frac{K^{-1}h_3}{\left\| K^{-1}h_1 \right\|} = \frac{K^{-1}h_3}{\left\| K^{-1}h_2 \right\|}, \quad (14)$$

where h_i is the i^{th} column vector of H. From the computed pose, the position of the vehicle can be finally determined from coordinate system transformation.

III. EXPERIMENTS

The proposed method was validated by using the actual field tests on the university campus. As shown in Fig. 3 (a), we chose two test sites, where the pavement lane lines were encoded for vehicle localization purpose. And a vehicle-borne monocular camera was used to capture the pavement images for localization (see Fig. 3 (b)). The angle of camera was configured so that it could observe at least two squares in the scene. Both the extrinsic and intrinsic parameters of the cameras were accurately calibrated in advance. In order to overcome the GPS-blind problems, we proposed using a WiFi fingerprint strategy for coarse localization. To serve this purpose, we disturbed AP base stations near the test sites.

(a)

(b)

Figure 3. (a) Two test sites on Yujiatou campus of WUT; (b) prototype intelligent vehicle for localization.

In the pavement coding step, we referred to the national road standards in China [16] for pavement geometry design. According the standards, pavement dash lines consists of a sequence of white squares. Each square has 2-meter long and 15-centimeters wide. Two adjacent squares have 2 meters apart. From such geometric configuration, the value E was computed as 3 by using (1). Therefore, we coded one square in yellow from a number of 3 squares, as shown in Fig. 4 (a).

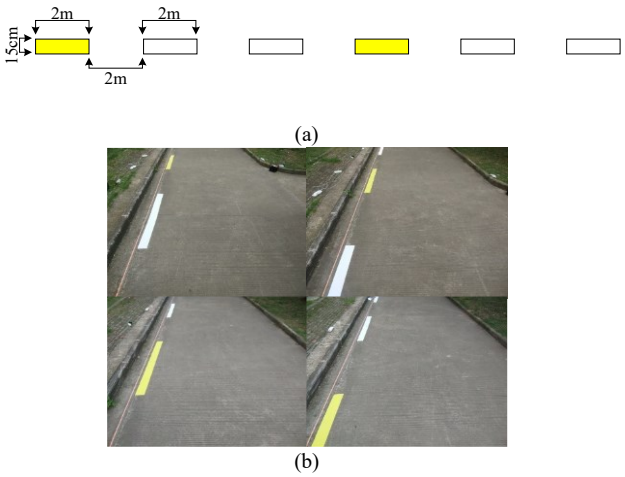

Figure 4. (a) Pavement lane coding from geometric configurations; (b) images of coded pavement markings.

In order to implement the proposed multi-scale localization method, we needed to pre-store some information for reference, a step also called mapping. For coarse localization, we partitioned the road areas into a number of cells and collected the WiFi fingerprints for all cells. As we also matched the local features around coded pavement marking, we stored all the extracted feature points together with their feature descriptors. From the camera calibration results, we could also compute the relative position between the coded pavement markings and the camera in the mapping process.

We first derived coarse localization results from WiFi fingerprint matching by using (3). Then, the real-time WiFi data collected by the vehicle were compared with those in different cells to achieve a coarse localization. The localization results of the two test sites are shown in the Fig. 5. It can be observed that the positioning errors from coarse localization are all less than 6.1 meters. From the coarse localization results in both sites, the mean and the standard deviation are 2.4 meters and 1.8 meters, respectively. Therefore, we can define the localization uncertainty as 4.2 meters (the mean plus the standard deviation). Hence, the coding value E in (1) can be computed as E=3. As a result, such coarse localization results allow us to derive a unique coded pavement marking (i.e., in yellow) from the image captured by the camera. From the coarse localization result, we can derive a set of candidate images within the range.

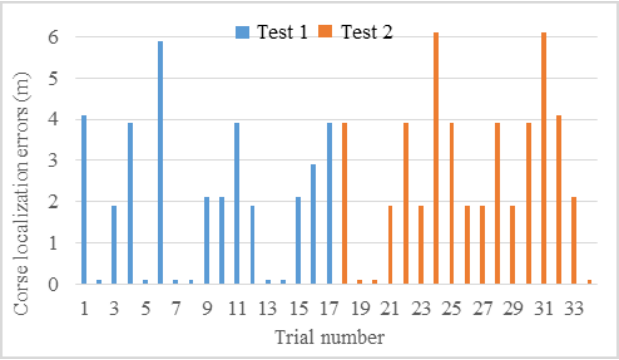

Figure 5. Coarse localization results from WiFi fingerprints.

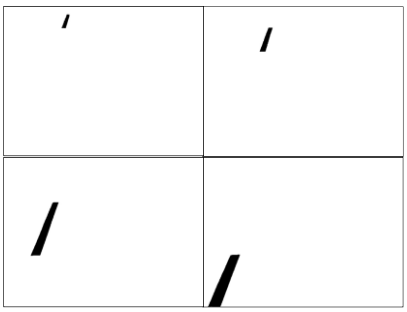

Figure 6. Detection results of pavement marking coded in yellow.

In the marking-level localization step, we detected pavement marking by using the proposed G-SCM model. From the G-SCM, all pixels in the query image were classified as yellow or non-yellow ones (as shown in Fig. 6). Hence, we could filter out all the yellow areas in the image, including the coded yellow markings. In addition, we also proposed using line detection and tracking to remove all the other yellow areas except the coded yellow markings. From the detection results, we could compute the distances between the camera and the coded pavement marking in candidate images from the camera calibration and pavement lane geometric configuration. As a result, we selected a unique image in the map, which had the least distance difference, as the marking-level localization result.

From the marking-level localization result, metric localization was finally performed to compute the relative pose of the vehicle-borne camera to the coded marking by matching distinctive visual feature points around the marking area, as shown in Fig. 7. Note that, this step can also enforce the matching between the query image and the image computed from marking-level localization. The relative poses were further converted into a global coordinate system from coordinate system transformation. The ground truths of the metric localization were obtained manually in the field. For each trial, we used the difference between the computed coordinates and the ground truths to evaluate the performance of the localization results. The results are illustrated in Fig. 8, where the results from different tests are marked in different colors. It can be observed that the positioning errors from metric localization are all less than 0.76 meters. From the localization results in both test sites, the mean and the standard deviation are all 0.5 meters and 0.1 meters respectively. The results demonstrate that the proposed method can raise the vehicle positioning accuracy to sub-meter based on multi-scale localization with robust performance.

Finally, the proposed method is also compared with some

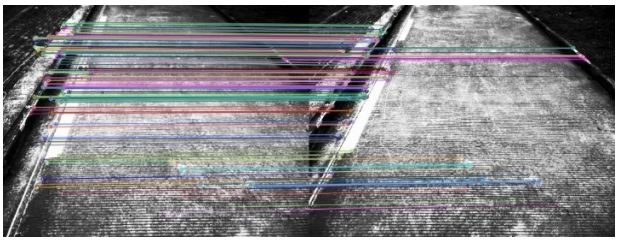

Figure 7. Image feature points matched between the query image and the candidate image.

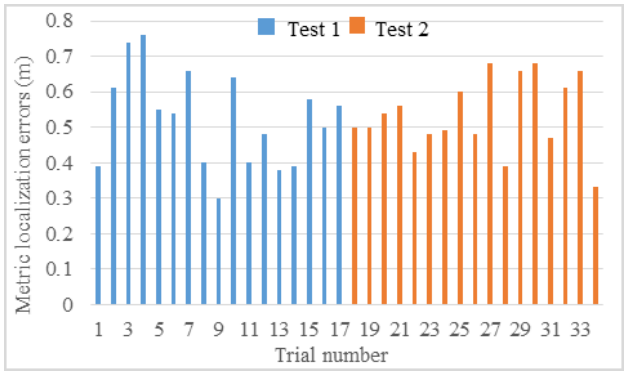

Figure 8. Metric localization results.

low-cost visual methods, which we have tested in the same condition. The results are illustrated in TABLE I, and it can be observed that the proposed method achieves sub-meter localization accuracy in real time, and has the best positioning accuracy and faster processing speed than other methods. Although the method in [8] has the fastest processing speed, it can only be used where there are outstanding marking without the requirement of changes to existing infrastructure, and its accuracy is worse than the proposed method. This means the proposed method is more advanced than other methods.

IV. Conclusions

This paper proposes a novel and accurate vehicle self-localization method by simply coding pavement lane lines. Thus both longitudinal and traverse position can be computed for vehicle self-localization, relative to traditional methods based on pavement lane lines. Therefore, the proposed method overcomes the limitations of existing vehicle localization approaches based on lane detection. In addition, this paper proposes a multi-scale localization strategy for coarse-to-fine position computation, which contributes to accurate vehicle localization. The proposed method has been validated in two field sites, where pavement lane lines were encoded in two different colors. Experimental results demonstrate that our method can achieve sub-meter level localization by simply coding pavement lanes. Based on the proposed method, we can utilize other vision-based methods to improve the positioning accuracy for real-time accurate vehicle localization.

TABLE I. Comparison Results of Different Methods for Vehicle Localization

Localization Methods	Hardware Setup	Mean Localization Error(m)	Mean Processing Time(ms)
Method in [1]	GNSS	3.4	1000
Method in [6]	Camera	4.0	510
Method in [8]	GPS+camera	3.6	50
Our method	**GPS+camera**	**0.5**	**150**

Acknowledgment

The work presented in this paper was funded by the National Natural Science Foundation of China (No.51679181), the Major Project of Technological Innovation of Hubei Province (No.2016AAA007), the Science-technology Programs Prior Funds for Overseas Chinese Talents of Hubei Province (No. 2016-12) and the Fundamental Research Funds for the Central Universities (No.2018III062GX).

References

[1] S. Miura, S. Hisaka, and S. Kamijo, "GPS multipath detection and rectification using 3D maps," in *Intelligent Transportation Systems (ITSC), 2013 16th International IEEE Conference on*, pp.1528-1534, IEEE, 2013.

[2] G. Gurusinghe, T. Nakatsuji, Y. Azuta, P. Ranjitkar, and Y. Tanaboriboon, "Multiple car-following data with real-time kinematic global positioning system," *Transportation Research Record Journal of the Transportation Research Board*, vol. 1802, no. 1, pp. 166-180, 2002.

[3] I. Bisio, M. Cerruti, F. Lavagetto, M. Marchese, M. Pastorino, A. Randazzo, and A. Randazzo, "A trainingless wifi fingerprint positioning approach over mobile devices," *Antennas and Wireless Propagation Letters, IEEE*, vol. 13, pp. 832-835, 2014.

[4] M. Kok, J. D. Hol, and T. B. Schön, "Indoor positioning using ultrawideband and inertial measurements," *Transactions on Vehicular Technology*, *IEEE*, vol. 64, no. 4, pp. 1293-1303, 2015.

[5] R. Faragher and R. Harle, "Location fingerprinting with Bluetooth low energy beacons," *Journal on Selected Areas in Communications*, *IEEE*, vol. 33, no. 11, pp. 2418-2428, 2015.

[6] J. Son, S. Kim, and K. Sohn, "A multi-vision sensor-based fast localization system with image matching for challenging outdoor environments," *Expert Systems with Applications*, vol. 42, no. 22, pp. 8830-8839, 2015.

[7] Z. Tao, P. Bonnifait, V. Fremont, and J. Ibanez-Guzman, "Lane marking aided vehicle localization," in *Intelligent Transportation Systems (ITSC), 2013 16th International IEEE Conference on*, pp. 1509–1515, IEEE, 2013.

[8] T. Wu and A. Ranganathan, "Vehicle localization using road markings," in *Intelligent Vehicles Symposium (IV)*, *2013 IEEE*, pp. 1185-1190, IEEE, 2013.

[9] J. H. Lim, K. H. Choi, J. Cho, and H. K. Lee, "Integration of GPS and monocular vision for land vehicle navigation in urban area," *International Journal of Automotive Technology*, vol. 18, no. 2, pp. 345-356, 2017.

[10] M. Schreiber, H. Konigshof, A. M. Hellmund, and C. Stiller, "Vehicle localization with tightly coupled GNSS and visual odometry," in *Intelligent Vehicles Symposium (IV), 2016 IEEE*, pp. 858–863, IEEE, 2016.

[11] G. Wan, X. Yang, R. Cai, H. Li, H. Wang, and S. Song, "Robust and precise vehicle localization based on multi-sensor fusion in diverse city scenes," *Arxiv Preprint*, Arxiv:1711.05805, 2017.

[12] Z. Zhang, "A flexible new technique for camera calibration," *Transactions on Pattern Analysis and Machine Intelligence*, *IEEE*, vol. 22, no. 11, pp. 1330-1334, 2000.

[13] H. Li, F. Nashashibi, and G. Toulminet, "Localization for intelligent vehicle by fusing mono-camera, low-cost GPS and map data," in *Intelligent Transportation Systems (ITSC)*, *2010 13th International IEEE Conference on*, pp. 1657-1662, IEEE, 2010.

[14] E. Rublee, V. Rabaud, K. Konolige, and G. Bradski, "ORB: An efficient alternative to SIFT or SURF," in *Computer Vision (ICCV), 2011 International IEEE Conference on*, pp. 2564 - 2571, IEEE, 2011.

[15] C. Song, H. Zhao, W. Jing, and H. Zhu, "Robust video stabilization based on particle filtering with weighted feature points," *Transactions on Consumer Electronics*, *IEEE*, vol. 58, no. 2, pp. 570-577, 2012.

[16] GB 5768.2-2009, "Road traffic signs and markings," *China: Standardization Administration of China*, 2009.